

Digital Scoring of Stromal Tumour Infiltrating Lymphocytes in Triple Negative Breast Cancer

Meenal Rawlani

A thesis

submitted in partial fulfillment of the

requirements for the degree of

Master of Science in Chemical Engineering

University of Washington

2024

Committee:

Shachi Mittal

Program Authorized to Offer Degree:

Chemical Engineering

© Copyright 2024

Meenal Rawlani

University of Washington

Abstract

Digital Scoring of Stromal Tumour Infiltrating Lymphocytes in Triple Negative Breast Cancer

Meenal Rawlani

Chair of Supervisory Committee:

Shachi Mittal

Department of Chemical Engineering

Accurate assessment of tumor-infiltrating lymphocytes (TILs), particularly in the stromal region, is a valuable prognostic and predictive biomarker in triple-negative breast cancer (TNBC). However, traditional scoring methods are subjective, labor-intensive, and lack standardization. This paper presents a computational pipeline for automated and quantitative evaluation of stromal TILs from whole slide images (WSIs) of pre surgery needle core biopsies of TNBC patients. The pipeline employs a multi-step approach, combining traditional image analysis techniques with deep learning models.

By combining traditional image analysis and deep learning approaches, the pipeline leverages the strengths of both methodologies to overcome the challenges of TIL quantification, including tissue heterogeneity and variability in TIL appearance and distribution. This work represents a significant step towards reliable and scalable TIL quantification, facilitating large-scale studies and enabling personalized treatment strategies based on TIL biomarkers.

Table of Contents

Chapter 1	INTRODUCTION	8
Chapter 2	DIGITAL SCORING OF STROMAL TUMOUR INFILTRATING LYMPHOCYTES IN TRIPLE NEGATIVE BREAST CANCER	11
2.1	Introduction.....	11
2.2	Methods.....	12
2.2.1	Patch Extraction	12
2.2.2	Three class classification and filtering.....	13
2.2.3	Stromal Mask	15
2.2.4	Superpatch.....	16
2.2.5	Clustering.....	17
2.2.6	Selection of the TIL Cluster.....	20
2.2.7	Filtering of TILs.....	21
2.2.8	TIL score.....	22
Chapter 3	RESULTS, DISCUSSION AND FUTURE DIRECTIONS	24

Table of Figures

Figure 2-1: An overview of the pipeline for the segmentation of TILs.	11
Figure 2-2: Numerous patches, as depicted here, of (4000,3000) px are extracted from WSI. ..	12
Figure 2-3: a) and c) are patches extracted from the WSI ; b) and d) are there corresponding classification such that each block of size (48,48) px is classified into either “stroma” depicted by red, “epithelium” depicted by blue and “others” depicted by green.	14
Figure 2-4: It is observed that a lot of rogue pixels in the stromal region of a) have been removed by the filtering in b). Similarly, the rogue blocks in both epithelial and stromal region seem to have been impacted significantly by the filtering.	15
Figure 2-5: The three-class classification was then used to isolate the stromal regions of the tissue as depicted in the figure. a) and c) are patches extracted from the WSI while b) and d) are the stromal tissue region masked out.	16
Figure 2-6: To capture the color variability in the stromal region better to further apply an unsupervised clustering algorithm, an image combining patches with different average RGB values was created. It is being referred to as the “superpatch.”	17
Figure 2-7: A 5-layer CNN model was trained to identify the TIL cluster	20
Figure 2-8: a) is the cluster containing TILs obtained after unsupervised clustering, b) is the TIL cluster after applying population density-based clustering c) is the patch extracted from WSI and d) is the TIL mask overlayed on the patch. e) and f) are zoom-ins	22
Figure 3-1: a) and c) are the patches extracted from WSI, b) and d) are the TIL mask overlayed on the patch. The pipeline is performing well in differentiating TILs from all the other kinds of cells in the TIL cluster.	24
Figure 3.2: A patch overlayed with DBSCAN model fit on the filtered TIL cluster. 8 distinct clusters were recognized by the model indicating the potential for identification of TIL sub-types.	26

ACKNOWLEDGEMENTS

First and foremost, I must express my profound gratitude to Prof. Shachi Mittal for giving me the invaluable opportunity to learn from her brilliance. Her unwavering standards for the caliber of work expected from her lab members have been an immense catalyst for my personal and professional growth. She has dedicated an extraordinary amount of time and mental bandwidth to ensure the success of this project, and I shall forever remain indebted to her. Her insightful feedback and ideas, week after week, have sculpted me into a far more confident engineer and researcher.

I am also deeply grateful to the very smart and very supportive members of the Mittal Lab, with whom I have embarked on a wonderful journey of learning and growth.

My sincere thanks extend to Dr. Anum K. for her encouraging words and invaluable feedback throughout this exhilarating process.

This thesis would not have been possible without the two trusty computers Luigi and Waluigi that rarely crashed, despite my relentless attempts to push their limits. Granted, they did succumb to a crash or two, but I swiftly fixed them, so let's keep that our little secret, shall we?

On a personal note, I am forever indebted to my parents, Bharat Kumar Rawlani and Sunita Rawlani, and my sister, Anushka Rawlani, for their unconditional love and unwavering encouragement in their own silly ways, even from the staggering distance of 7,538 miles. They have made countless sacrifices throughout my academic journey, and their belief in me has been an unparalleled source of motivation.

I am also profoundly grateful to my friends, Mehak, Manjari, Prithvi, Prachi, Fatwir, Jyo, Shubsie, Kammy, Hemanth, and Akshat, who have been my family away from home. Their emotional support during those two days before the group meeting, every week, was the sole reason I have reached this far.

I would like to conclude with a simple yet powerful reminder:

"Never apologize for success."

Chapter 1

INTRODUCTION

Triple-negative breast cancer (TNBC) is a rare but biologically aggressive and heterogenous subtype of breast cancer marked by the lack of expression of estrogen receptor (ER), progesterone receptor (PR), and human epidermal growth factor receptor 2 (HER2). This makes the treatment options for TNBC patients very limited. Due to the lack of these receptors, patients do not respond to hormonal therapies and HER2-targeted therapies. This has led to chemotherapy being the cornerstone of treatment for most TNBC patients. (Zagami et al., 2022; Ribeiro et al., 2022)

Tumor Infiltrating Lymphocytes are immune cells, primarily T cells, B cells and natural killer cells, which migrate from the bloodstream and infiltrate the tumor microenvironment (TME) (Wu et al., 2023). These cells can recognize and attack tumor cells, making them a significantly important component of the body's defense against cancer (Gonzalez et al., 2018). TILs can be further categorized into two categories, intratumoral TILs and stromal TILs. As the name suggests, intra-tumoral clusters are found within tumor clusters while stromal TILs are found in the stroma surrounding the tumor clusters (Kazemi et al., 2022). Stromal TILs have been shown to be a strong prognostic and predictive biomarker in TNBC, with higher levels associated with improved pathological complete response rates to neoadjuvant chemotherapy and better overall survival (Loi et al., 2019). Accurate assessment of stromal TILs in pre-treatment TNBC biopsies could assist in the stratification of patients, treatment selection, and identifying candidates for immunotherapeutic interventions (Ciarca et al., 2024).

The presence and density of TILs have been recognized as important biomarkers in cancer, however their assessment has relied on semi-quantitative scoring methods by pathologists, which are subjective and prone to inter-observer variability (Salgado et al., 2015). The lack of a quantitative method for the evaluation of TILs has been a significant obstacle in the widespread clinical implementation. It also limits the ability to compare the observations made by various studies. (Tine et al., 2023)

The International TILs Working Group has been working to develop and validate standardized methodologies for TIL assessment (Salgado et al., 2015; Hendry et al., 2017). Their efforts have focused on developing a consistent and reproducible scoring system for TILs in tumors, particularly in breast cancer. The group has proposed assessing the stromal and intratumoral TIL compartments separately, reporting TIL levels as a continuous parameter (percentage of stromal or tumor area occupied by TILs) rather than categorical scores. (Salgado et al., 2015; Hendry et al., 2017).

While these guidelines are helpful, there are several obstacles in achieving a truly quantitative and automated assessment of TILs. Manual scoring is time-consuming, labor-intensive, and subjective, limiting its scalability for large-scale studies or clinical implementation (Klauschen et al., 2018). Inter-observer variability persists even with standardized guidelines, highlighting the need for reproducible quantification methods (Salgado et al., 2015). Additionally, TILs exhibit significant spatial heterogeneity within tumors, and sampling from limited tissue sections may not accurately represent the overall TIL distribution (Khoury et al., 2018).

To overcome these challenges, there have been various attempts at computational methods for automated quantification of TILs from WSIs (Saltz et al., 2018; Klauschen et al., 2018; Thagaard et al., 2023; Bai et al., 2021). These methods can be broadly categorized into two main approaches: traditional image analysis techniques and deep learning-based methods.

Several studies have employed traditional image analysis techniques, such as color decomposition, segmentation, and morphological operations, to quantify TILs in WSIs. These methods typically involve separating the hematoxylin and eosin (H&E) stained image into individual color channels to enhance the contrast between different tissue components, identifying and segmenting individual nuclei based on shape, size, and color characteristics, extracting morphological and textural features from the segmented nuclei to distinguish lymphocytes from other cell types. Then using machine learning algorithms, such as support vector machines (SVMs) random forests or artificial neural networks (ANN), to classify the segmented nuclei as lymphocytes or non-lymphocytes based on the extracted features (Saltz et al., 2018; Lim et al., 2023). While these traditional methods have shown promising results, they often rely on carefully designed and tuned feature extraction and classification pipelines, which

can be time-consuming and may not generalize well across different tissue types or staining protocols (Saltz et al., 2018; Klauschen et al., 2018).

With the recent advancements in deep learning, particularly in the field of computer vision, researchers have explored the use of convolutional neural networks (CNNs) for automated TIL quantification. These methods typically involve training a CNN model on annotated WSI patches to directly classify image regions as containing TILs or not. Some examples of deep learning-based approaches include patch-based classification, dividing the WSI into small patches and training a CNN to classify each patch as containing TILs or not (Corredor et al., 2019); semantic segmentation, training a CNN to perform pixel-wise segmentation of the WSI, identifying regions containing TILs (Lu et al, 2020); and instance segmentation, training a CNN to not only identify TIL regions but also segment individual lymphocytes (Liu et al., 2022; Choi et al., 2023). Deep learning-based methods have shown promising results and can potentially capture complex patterns in the data, they also have various drawbacks. The requirement for a substantial amount of accurately annotated data, which can be time-consuming and expensive to obtain (Yosofvand et al., 2023). The black box nature of these algorithms results in limited interpretability, making it difficult to understand the decision-making process and identify potential biases (Hayashi et al., 2019). Generalization challenges, where models trained on data from a specific institution or staining protocol may not generalize well to data from other sources, limiting their broader applicability (Hassouna et al., 2023). Computational resource requirements, as training and deploying deep learning models can be computationally intensive, requiring specialized hardware and resources (Klauschen et al., 2018).

Chapter 2

DIGITAL SCORING OF STROMAL TUMOUR INFILTRATING LYMPHOCYTES IN TRIPLE NEGATIVE BREAST CANCER

2.1 Introduction

The pipeline starts by extracting manageable image patches from massive WSIs obtained from pre-surgery biopsies. The trained VGG-19 model was retrained to classify tissue regions within the patches into epithelium, stroma, and others, with a contextual filtering approach to refine the results. Binary masks are created to isolate the stromal patches where TILs reside. A superpatch is created to capture the color variability and broader context within the WSI by stitching heterogenous patches. K-means clustering is applied to the superpatch, identifying four distinct clusters, including one containing TILs. A separate CNN model is trained to pinpoint the TIL cluster automatically. Finally, population-based filtering is applied to distinguish TILs from visually similar fibroblasts through filtering techniques. The overall approach is outlined in Fig. 2-1.

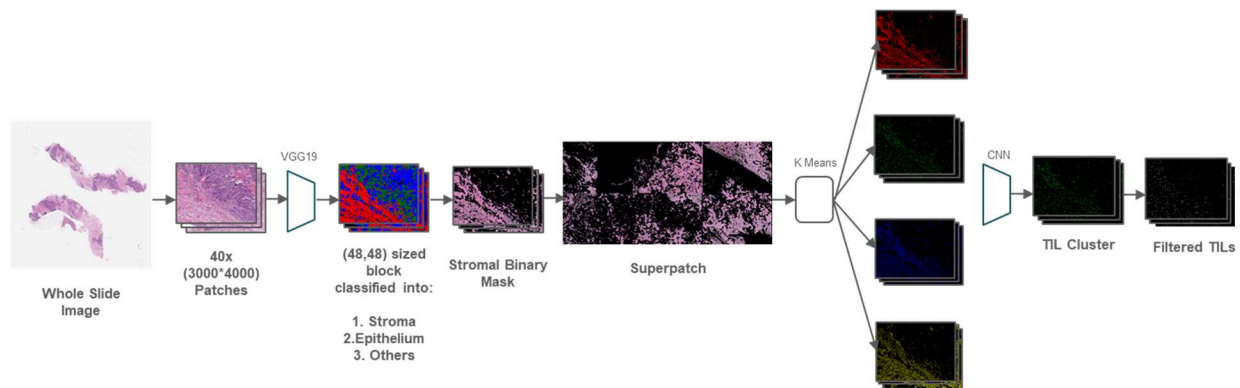


Figure 2-1: An overview of the pipeline for the segmentation of TILs.

2.2 Methods

2.2.1 Patch Extraction

In the development of an automated computational pipeline for the assessment of whole slide images (WSIs), an important preprocessing step is the extraction of image patches since the WSIs are massive and extremely feature-rich to be directly fed into machine learning algorithms. To overcome this challenge, smaller image patches are extracted from the WSIs based on user-provided annotations.

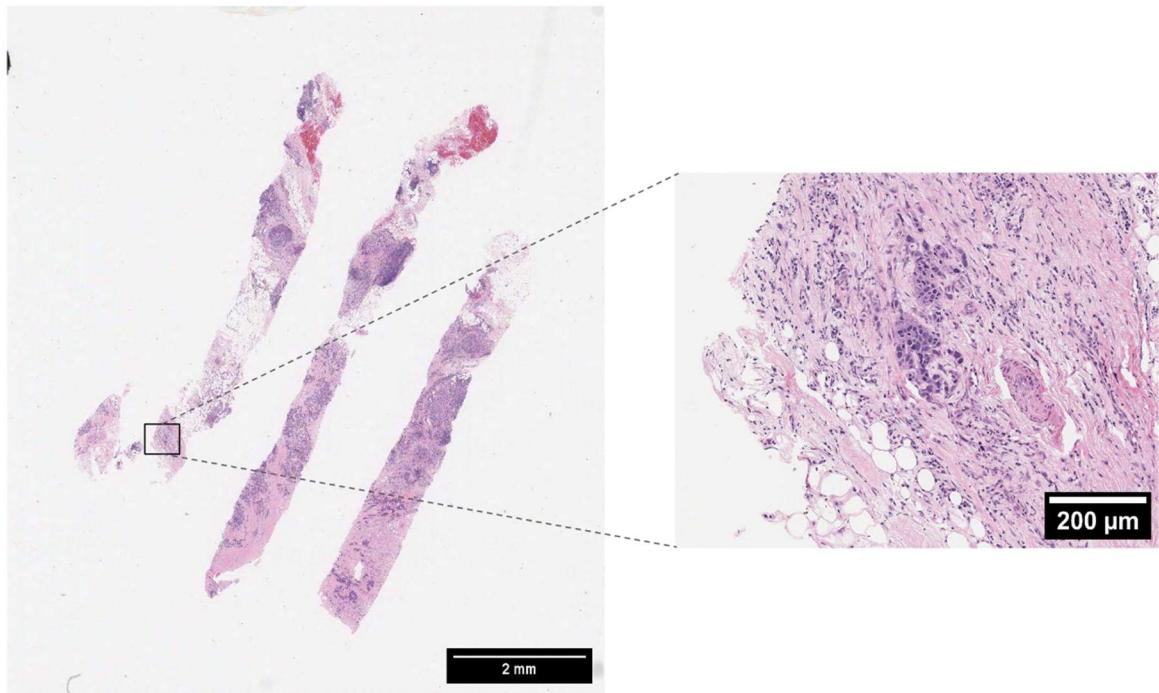


Figure 2-2: Numerous patches, as depicted here, of (4000,3000) px are extracted from WSI.

Specifically, users can draw free-hand annotations around regions of interest, and as depicted in Fig. 2-2; patches of size (4000, 3000) px are extracted, with a 5% overlap and 5% padding between adjacent patches. The choice of the patch size (4000, 3000) px was a carefully considered trade-off between the number of patches generated and the computational ease of processing. While larger patch sizes would reduce the total number of patches, they would also increase the memory requirements for each analysis step. Conversely, smaller patch sizes would generate a larger number of patches, potentially capturing finer details but also increasing the computational complexity. The selected patch size is such that it provides sufficient resolution

and context while also ensuring manageable processing requirements. The decision to include overlap and padding between patches is to ensure that tissue regions, particularly those at the boundaries, are not missed during the extraction process. This approach helps to capture the context and continuity of the tissue.

During the process of extraction, thresholding is used to exclude irrelevant background areas from the extracted patches. The patches are converted to grayscale and then pixels with color values between 200 and 255 are identified as background pixels. If more than 70% of the pixels in a patch fall within this range, the entire patch is considered background and not analyzed further. This range was decided empirically, through multiple iterations, ranging from 65% to 90%. The aim was to obtain a threshold such that the essential tissue regions are retained but the inclusion of irrelevant background areas is minimized, which could potentially introduce noise and affect the performance of the downstream tasks. With this preprocessing step, a set of relevant image patches are obtained, ready for analysis in the computational pipeline.

2.2.2 Three class classification and filtering

Once the relevant image patches have been extracted from the whole slide images (WSIs), the next steps focus on isolating the stromal regions, as these areas are of particular interest for sTILs. To achieve this, a pretrained VGG-19 model was applied. (Mittal et al., 2019)

The choice of VGG-19 was motivated by its ability to process input tiles as small as (48,48) px, enabling a more granular classification within the image patches. Smaller input tiles lead to a higher spatial resolution in the classification output, capturing finer details and reducing the risk of smoothing out localized tissue patterns. By analyzing each (48,48) px block within a patch, the VGG-19 model classifies the tissue into three categories: “epithelium”, “stroma”, and “others.”

The model was retrained on patches extracted from 6 WSIs from the Triple-Negative Breast Cancer (TNBC) cohort. Patches of sizes of (256,256) px and (48,48) px were used to encapsulate regions at multiple zoom levels, providing the model with the ability to analyze WSIs like a pathologist.

During retraining, only the last two fully connected layers were retrained using a total of 3000 patches per class from multiple zoom levels. The data was split into 70% for training, 20% for

validation, and 10% for testing. To incorporate more data and capture shifts in tissue regions, data augmentation was used, including shear range of 0.2, zoom range of 0.2, rotation range of 20 degrees, width and height shift ranges of 0.2, and horizontal flipping.

A total of 528,387 parameters were trainable. The model monitored validation accuracy for early stopping with a patience of 10 epochs. Additionally, ReduceLRonPlateau was used to monitor validation accuracy, with a factor of 0.1 and a patience of 5 epochs. The training was performed for 50 epochs.

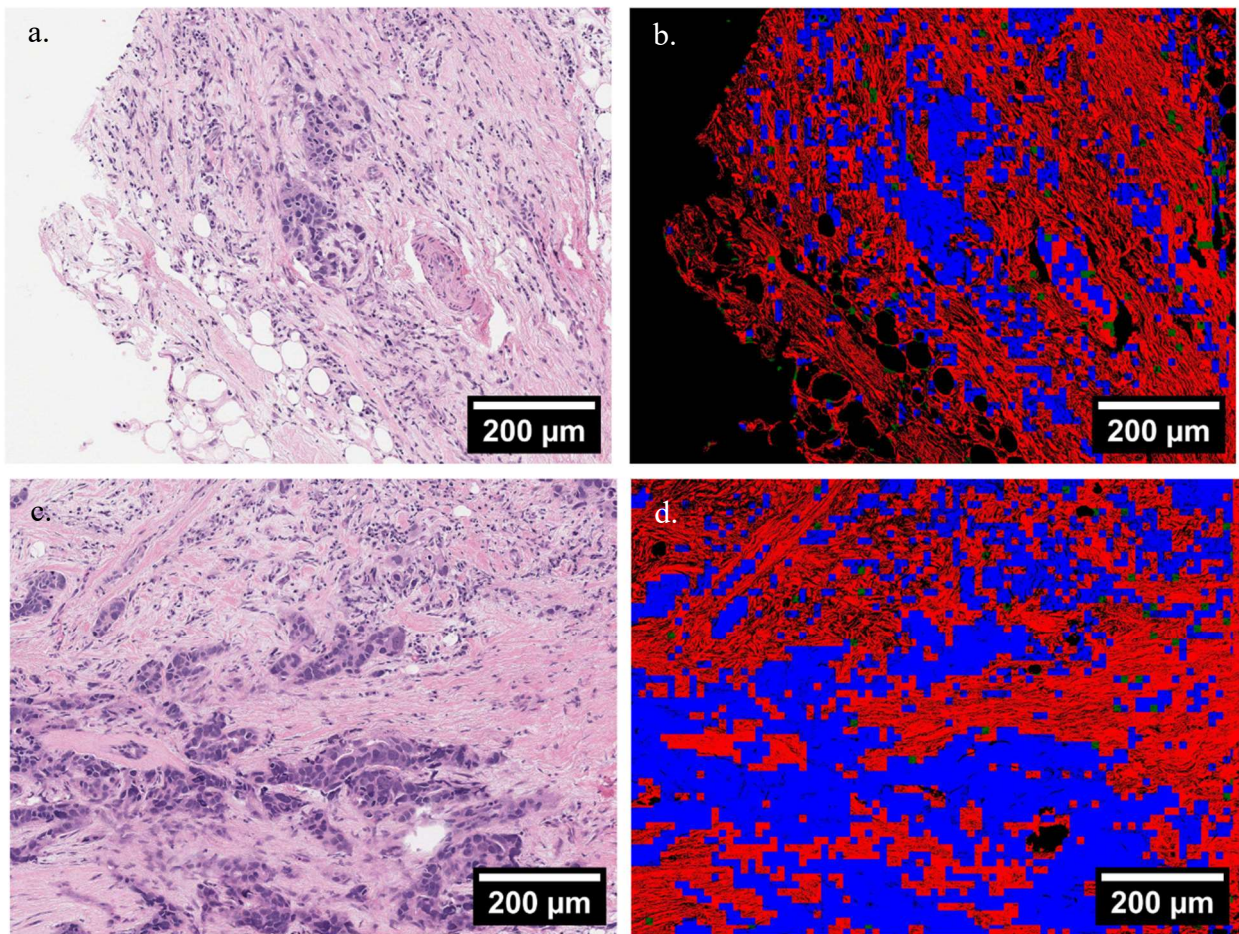


Figure 2-3: a) and c) are patches extracted from the WSI ; b) and d) are there corresponding classification such that each block of size (48,48) px is classified into either “stroma” depicted by red, “epithelium” depicted by blue and “others” depicted by green.

After retraining, the model achieved a test accuracy of 97.31%. Fig. 2-3 depicts the application of the retrained model on two patches.

However, when using a model trained by transfer learning, potential misclassifications that may arise due to the heterogeneity of the tissue need to be taken care of. For example, if a region within a patch is epithelial, with a single stromal block, this block is most likely misclassified by the model.

As a result, a filtering approach was developed and implemented that was based on neighborhood context. A sliding window of size (144,144) px was applied around each (48,48) px block. If the block at the center did not belong to the majority class, the classification is changed to match the majority class within the window. Fig. 2-4 highlights the changes seen in the patch after contextual filtering.

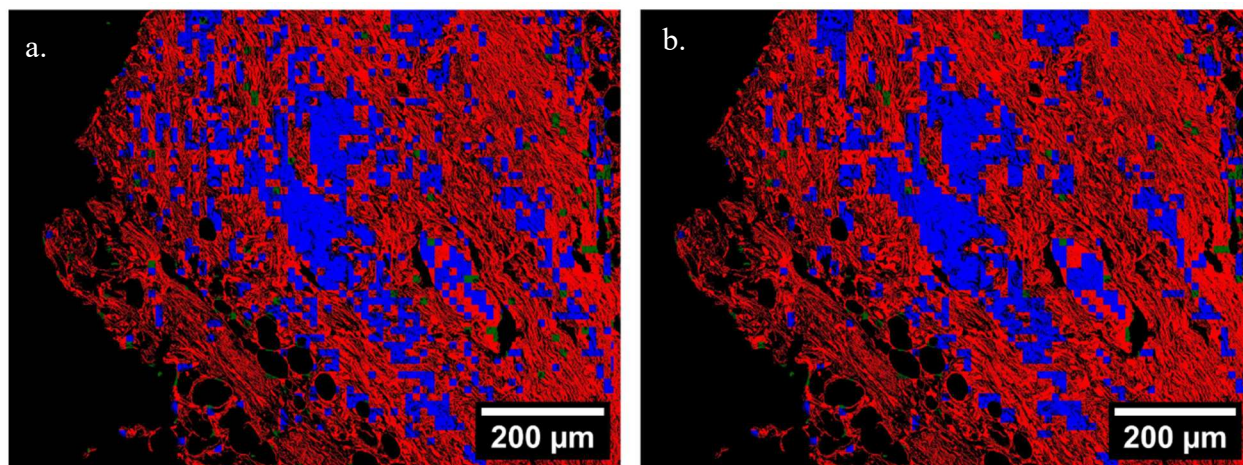


Figure 2-4: It is observed that a lot of rogue pixels in the stromal region of a) have been removed by the filtering in b). Similarly, the rogue blocks in both epithelial and stromal region seem to have been impacted significantly by the filtering.

2.2.3 Stromal Mask

After applying filtering to refine the tissue classification results obtained from the VGG-19 model, the next step in the computational pipeline is to focus on the stromal regions, which are of particular interest for identifying and quantifying tumor-infiltrating lymphocytes (TILs). To achieve this, binary masks were created for each patch, where all the pixels that are classified as “epithelium” or “others” are masked out, leaving only pixels classified as “stroma.” This effectively extracts the region of interest, stroma, for effective segmentation for TILs downstream. Fig. 2-5 depicts the extracted stromal region for two patches.

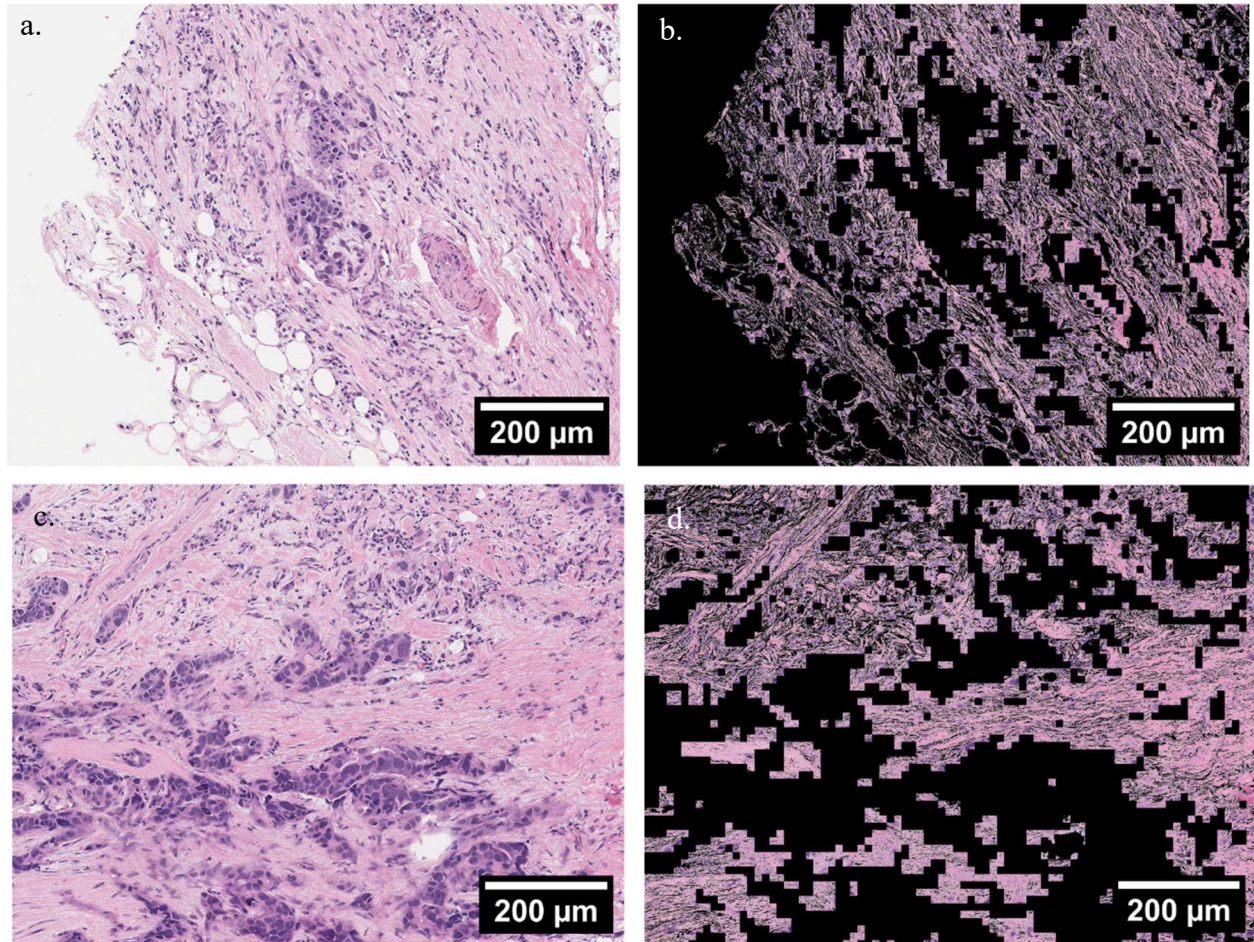


Figure 2-5: The three-class classification was then used to isolate the stromal regions of the tissue as depicted in the figure. a) and c) are patches extracted from the WSI while b) and d) are the stromal tissue region masked out.

2.2.4 Superpatch

Clustering directly on individual patches from whole slide images (WSIs) often encounters challenges such as high computational complexity and failure to capture the broader context and color variability present in the entire image. To address these limitations, a superpatch approach is introduced, aiming to construct comprehensive representations of the WSI. This superpatch is formed by quantitatively sampling representative patches from diverse color distributions across the WSI, thereby adapting to staining variations and ensuring a more accurate portrayal of biological heterogeneity. By incorporating broader context analysis, this approach enhances the

robustness and effectiveness of clustering algorithms in capturing the complex spatial and color relationships within WSIs, facilitating more nuanced and insightful analysis in digital pathology.

The stromal region and subsequently the TILs exhibit significant variability in their appearance and distribution within the tumor microenvironment (Yuan, 2016; Saltz et al., 2018). Therefore, to capture this variability, a superpatch is used. The superpatch is a condensed representation of the color variation present within the original whole slide image (WSI), made by combining selected patches from different regions of the tissue. Specifically, the average RGB pixel values for each patch from a WSI are calculated and stored in a data frame. These patches are then segregated into six bins based on their color characteristics. From each bin, a representative patch is chosen, and these selected patches are stitched together to form the superpatch. Fig. 2-6 depicts the superpatch obtained for a WSI.

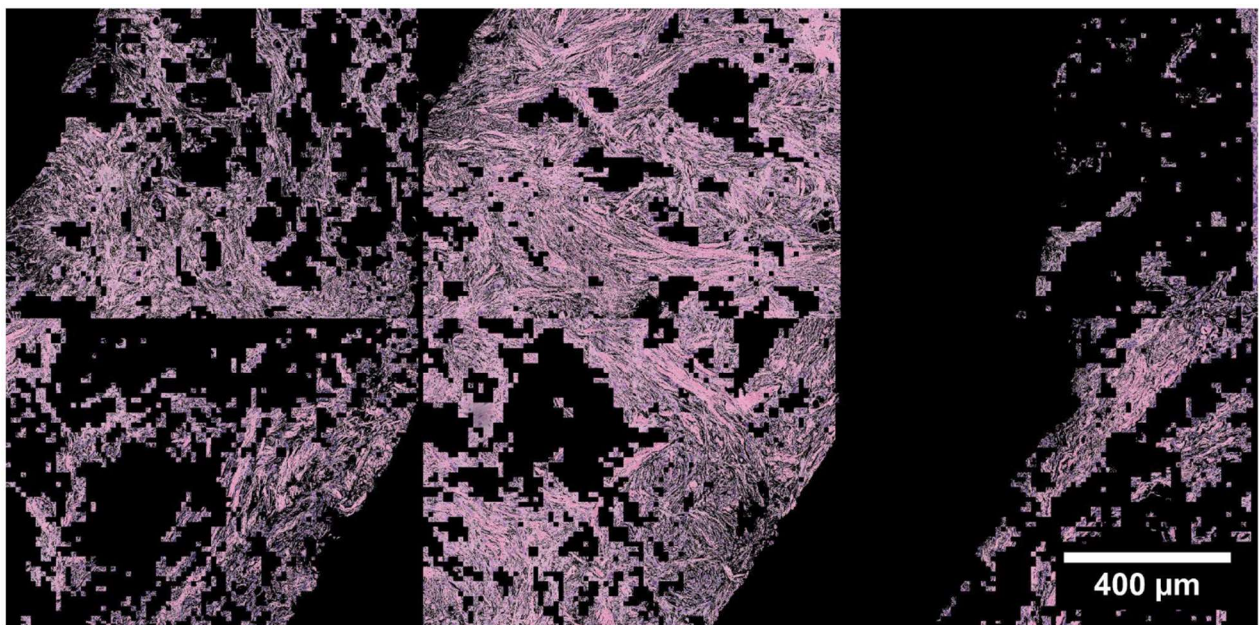


Figure 2-6: To capture the color variability in the stromal region better to further apply an unsupervised clustering algorithm, an image combining patches with different average RGB values was created. It is being referred to as the “superpatch.”

2.2.5 Clustering

Applying clustering algorithms directly on individual patches would be computationally intensive and might fail to capture the broader context of color variations, leading to suboptimal

results. By leveraging the superpatch, the pipeline can analyze the color variations and patterns within a single, manageable representation of the entire WSI.

Subsequently, a k-means clustering model is fitted on the superpatch, with the number of clusters determined by examining the elbow point in the inertia plot, as depicted in Fig. 2-8. In this implementation, four distinct clusters are identified: two clusters representing fibrous structures, potentially corresponding to collagen fibers or dense connective tissue; one cluster containing tumor-infiltrating lymphocytes (TILs), fibroblasts, plasma cells, and misclassified epithelial cells; and one cluster representing edge artifacts or boundary regions.

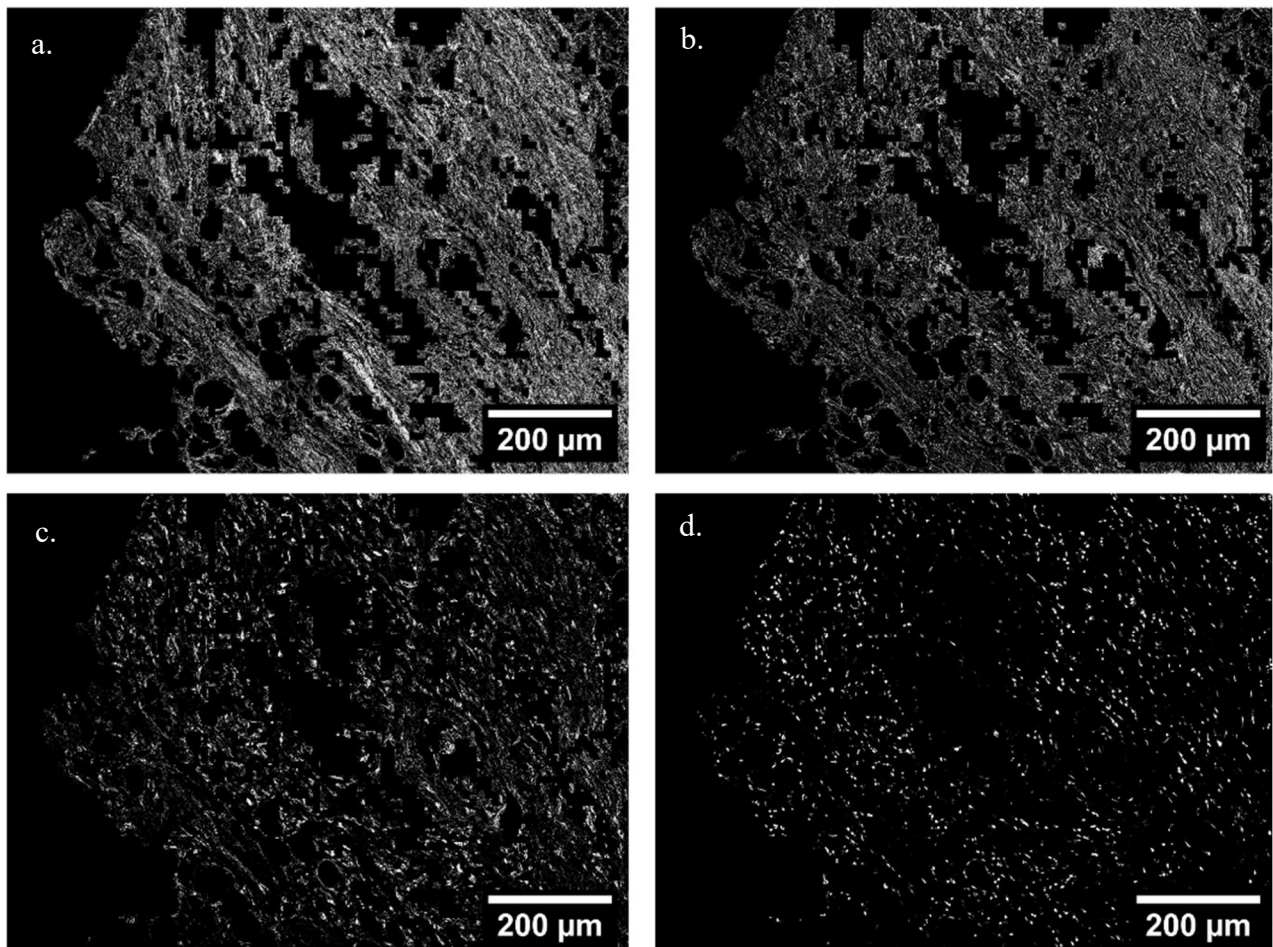


Figure 2.7: a) and b) represent the fibrous structures c) is the edge class for the TIL cluster while d) represents the cluster containing TILs.

The presence of two distinct clusters containing fibrous structures highlights the ability of the clustering algorithm to capture the diverse morphological features present within the tumor microenvironment. These fibrous clusters, as shown in Fig. 2-7 a. and b., may correspond to collagen fibers or dense connective tissue, which are known to play important roles in tumor progression, metastasis, and immune cell infiltration (Maller et al., 2010).

Importantly, one of the clusters, as shown in Fig. 2-7 d., identified by the k-means algorithm encompasses TILs, the primary cells of interest for quantification in this pipeline. However, it is noteworthy that this cluster also includes other cell types, such as fibroblasts, plasma cells, and potentially misclassified epithelial cells. This observation underscores the complexity and heterogeneity of the tumor microenvironment, where various cell types can exhibit similar morphological and staining characteristics, making it challenging to achieve a perfect separation based solely on unsupervised clustering techniques.

The last cluster identified by the k-means algorithm is designated as an edge class, as shown in Fig. 2-7 c., representing artifacts or boundary regions within the superpatch. The inclusion of this cluster helps to account for potential edge effects or irregularities that may arise during the image stitching process or due to variations in tissue preparation and staining

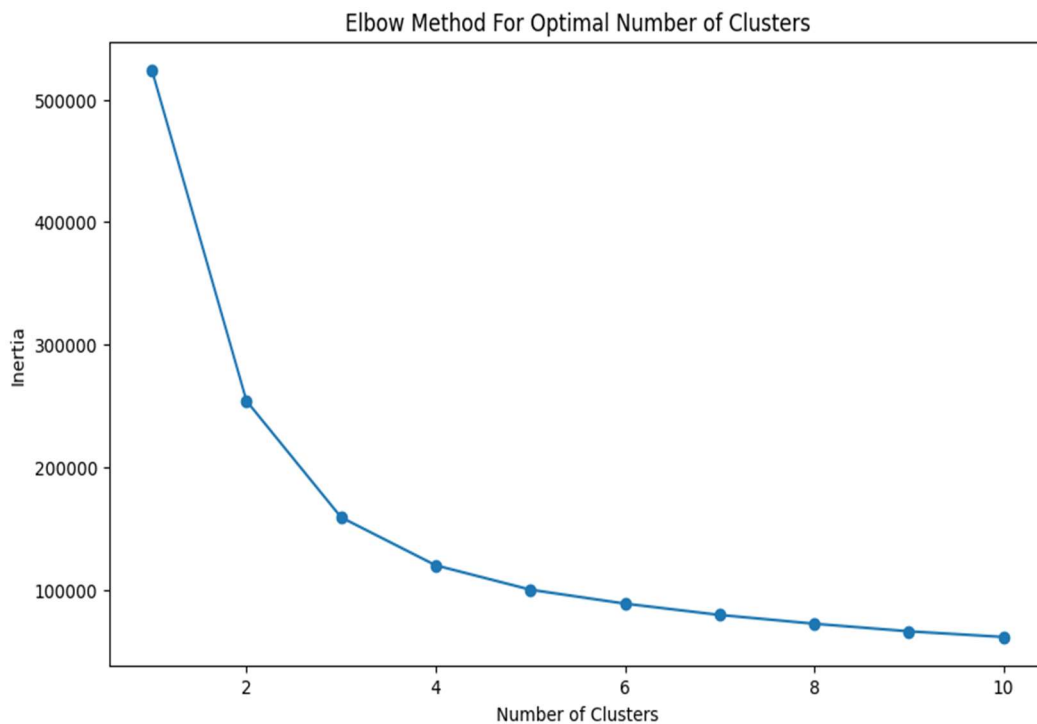


Figure 2-8: KMeans model was fit on the superpatch and the inertia for each cluster was calculated. The elbow point occurs when the number of clusters is 4.

While k-means clustering has been widely used for unsupervised pattern recognition and data partitioning (Jain, 2010), its application in the context of TIL quantification is novel and tailored to capture the specific characteristics of TILs within the tumor microenvironment.

2.2.6 Selection of the TIL Cluster

Conventionally, the identification of the target cluster after applying clustering algorithms like k-means has relied on visual inspection by human experts. However, this manual approach hinders the development of a truly automated and standardized pipeline for TIL quantification. To address this challenge and minimize manual intervention, we developed a dedicated CNN model specifically tailored for the automated identification of the TIL cluster. This CNN model takes the folder containing the four clusters generated by the KMeans as input and selects the cluster that contains TILs. The architecture of the CNN model is as follows:

1. Two convolutional layers with 32 and 64 filters, respectively, each followed by max pooling operations.

Convolutional layers are effective in extracting local features and patterns from image data (Krizhevsky et al., 2012).

2. This layer flattens the output of the convolutional layers, preparing the data for the fully connected layers.

3. Two dense layers, with the first layer having 64 units and a ReLU activation function, followed by a second layer with a single unit and a sigmoid activation function for binary classification.

The CNN model was trained on a dataset consisting of 600 patches extracted from four different WSIs, with a 70-20-10 split for train, validation, and test sets, respectively. It is compiled using

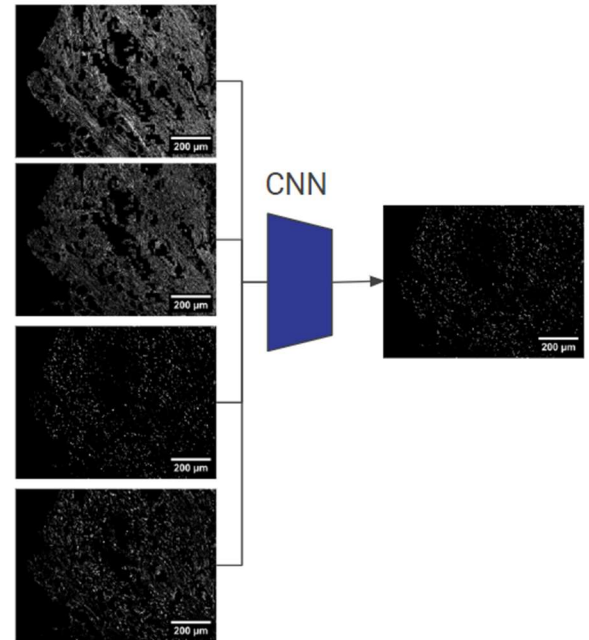


Figure 2-9: A five-layer CNN model was trained to identify the TIL cluster from the four clusters produced through KMeans

Adam optimizer, with the binary cross-entropy loss function and accuracy metric for performance evaluation.

To prevent overfitting and improve generalization, an EarlyStopping callback is implemented, which monitors the validation accuracy during training. If the validation accuracy does not improve for four consecutive epochs, the training process is stopped.

After retraining, the model achieved a test accuracy of 96.06 %.

The confidence in the model's prediction was further enhanced during the TIL cluster identification process by employing a majority voting system. Multiple patches were considered from each cluster during the identification of the TIL cluster to reduce the impact of outliers and ambiguous instances.

The voting mechanism is implemented as follows:

1. Patch Selection: For each cluster under consideration, three patches are randomly sampled.
2. Individual Patch Classification: Each of the patches independently underwent binary classification to determine whether it contains TIL.
3. Majority Vote: If at least two out of the three patches are classified as containing TIL, that cluster is labeled as TIL cluster.

2.2.7 Filtering of TILs

After identifying the cluster containing tumor-infiltrating lymphocytes (TILs), it is crucial to distinguish TILs from other cell types present within the same cluster, such as plasma cells, fibroblasts, and misclassified epithelial cells. To achieve this, we used filtering based on morphological features, including area, perimeter, and circularity.

Fibroblasts are known to exhibit an elongated morphology compared to TILs (Ravikanth et al., 2011). This morphological difference was utilized in the form of a circularity filter to eliminate fibroblasts from the identified cluster. Circularity is a measure of how closely a shape resembles a circle, with a value of 1 representing a perfect circle. By setting circularity thresholds such that

only contours with a circularity greater than 0.45 were included, the elongated fibroblasts were distinguished from the more rounded TILs.

Epithelial cells, which may be misclassified into the stromal region, typically have larger dimensions compared to TILs. By defining suitable thresholds for area and perimeter, misclassified epithelial cells were effectively separated from the desired TIL population based. As highlighted by Fig. 2-10,

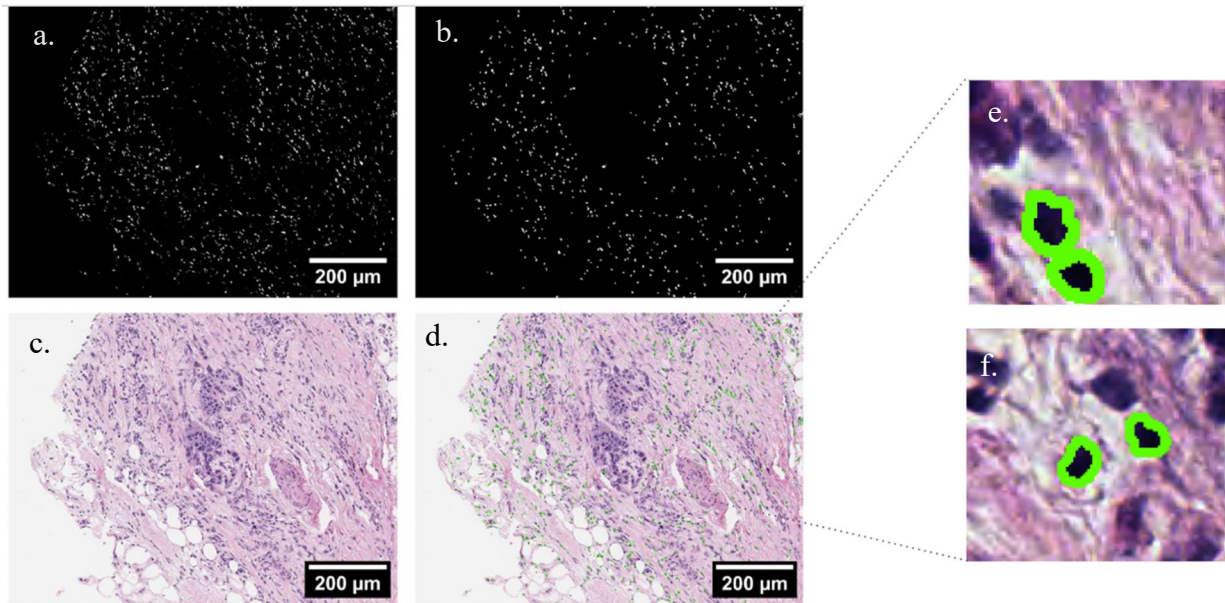


Figure 2-10: a) is the cluster containing TILs obtained after unsupervised clustering, b) is the TIL cluster after applying population density-based clustering c) is the patch extracted from WSI and d) is the TIL mask overlaid on the patch. e) and f) are regions of d. zoomed-in to get a detailed view of TILs.

2.2.8 TIL score

Accurate quantification of tumor-infiltrating lymphocytes (TILs) in breast cancer is crucial but challenging due to potential misclassification of larger epithelial tumor cells into the stromal region. Since the VGG-19 model classified epithelial cells into a separate class and further the filtering of the TIL containing cluster excluded the epithelial cells, TIL scores were calculated as the ratio of TIL area to stromal area, per TIL Working Group guidelines. The stromal area is obtained from the binary stromal masks created earlier in the pipeline. The total stromal area is calculated by summing the stromal pixel counts across all patches. The filtered TIL cluster

provides the TIL pixel locations. The TIL area is calculated by summing the TIL pixel counts across all patches. The TIL score represents the percentage of the stromal area occupied by TILs.

The pipeline has been built in such a way that it is user-agnostic and platform-independent. Users can simply input a folder containing multiple whole slide images (.svs) and the annotated region of interest (.xml) No additional user intervention is required. The pipeline is designed to be agnostic of the underlying operating system. It can run seamlessly on Windows, macOS, or Linux systems.

Chapter 3

RESULTS, DISCUSSION AND FUTURE DIRECTIONS

The pipeline demonstrates promising capabilities in identifying tumor-infiltrating lymphocytes (TILs) upon visual inspection.

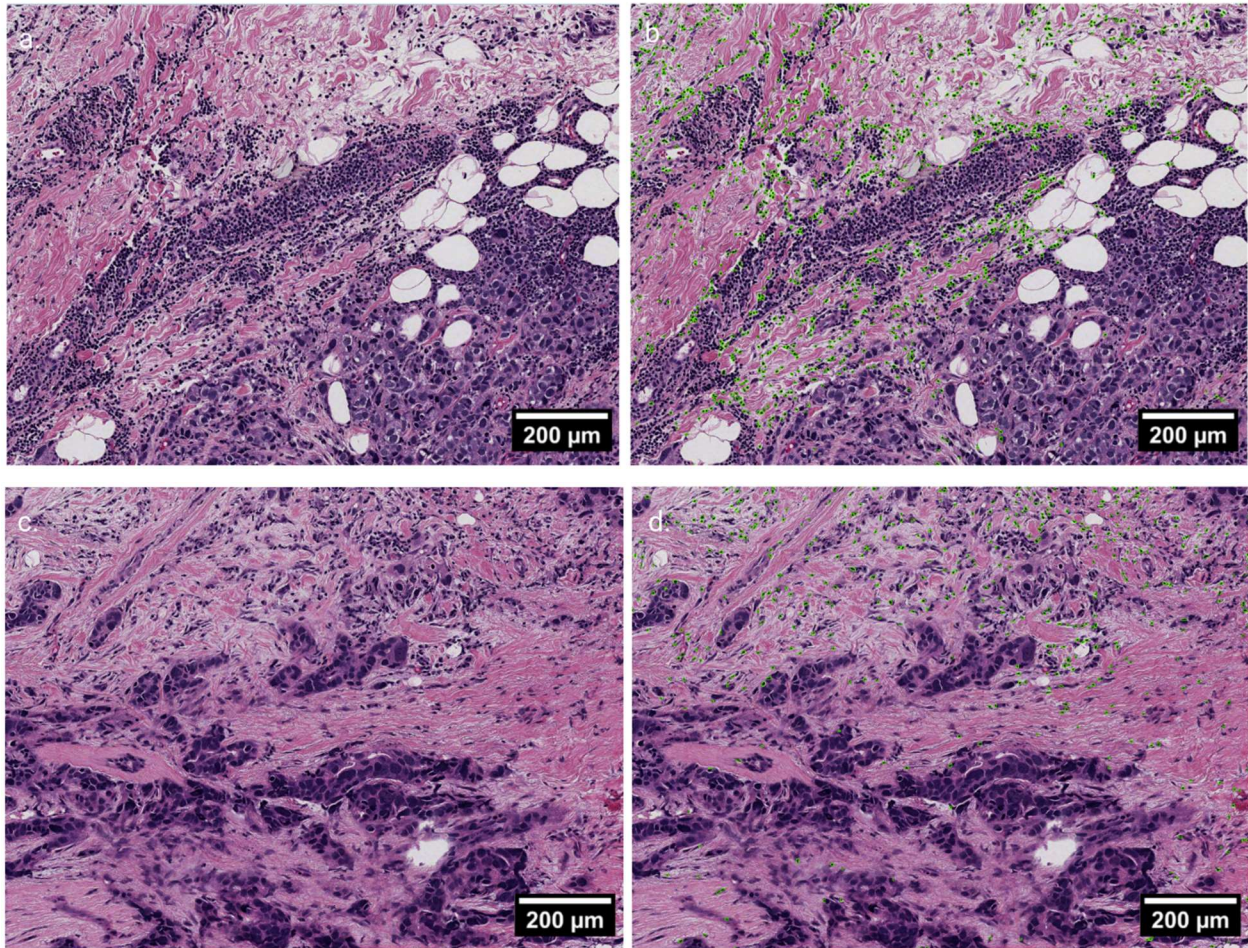


Figure 3.1: a) and c) are the patches extracted from WSI, b) and d) are the TIL mask overlaid on the patch. The pipeline is performing well in differentiating TILs from all the other kinds of cells in the TIL cluster.

Our preliminary assessment indicates that the pipeline can accurately identify TILs, laying a solid foundation for further investigation. However, a comprehensive statistical analysis was hindered by the limited availability of patient data.

Despite this limitation, our pipeline represents a promising approach to TIL assessment in breast cancer. By integrating efficient machine learning and image segmentation techniques, we have developed a robust methodology for TIL identification. Notably, our approach holds particular

significance in the context of triple-negative breast cancer (TNBC), as it has the potential to provide novel insights into TNBC prognosis through TIL analysis.

A recent study (Liu et al., 2023) introduces an innovative approach for tumor-infiltrating lymphocyte (TIL) assessment, utilizing U-Nets and a publicly annotated dataset. While their methodology demonstrates significant advancements in TIL analysis, the computational complexity of their model results in significant processing time. For instance, calculating the TIL score based on even a portion of the whole slide image can take up to three hours. This prolonged processing time may hinder scalability and efficiency in clinical settings, where timely analysis is crucial for patient care. Additionally, despite labeling various semantic regions as TILs, the cellular segmentation does not consistently align with these regions. TILs are found outside the labeled semantic regions, suggesting potential inaccuracies or limitations in the segmentation approach.

Based on this work, the following three tasks will be carried out:

1. **Survival Analysis and Clinical Validation:** We have developed a pipeline for generating Kaplan-Meier survival curves based on the quantified TIL scores. Our next step involves validating the prognostic significance of the automated TIL assessment by applying this pipeline to a larger patient cohort. This will enable us to obtain more robust and clinically meaningful results, enhancing the prognostic value of our method in clinical settings.
2. **Exploring TIL Heterogeneity with DBSCAN:** To gain deeper insights into the heterogeneity within the identified TIL clusters, we are employing DBSCAN (Density-Based Spatial Clustering of Applications with Noise) clustering. As shown in Fig. 3-2, this approach will enable us to investigate potential sub-clusters or variations among different lymphocyte populations within the TIL clusters. Understanding these sub-clusters will provide a more

nuanced understanding of their morphological and functional diversity, which could lead to more targeted and effective therapeutic strategies.

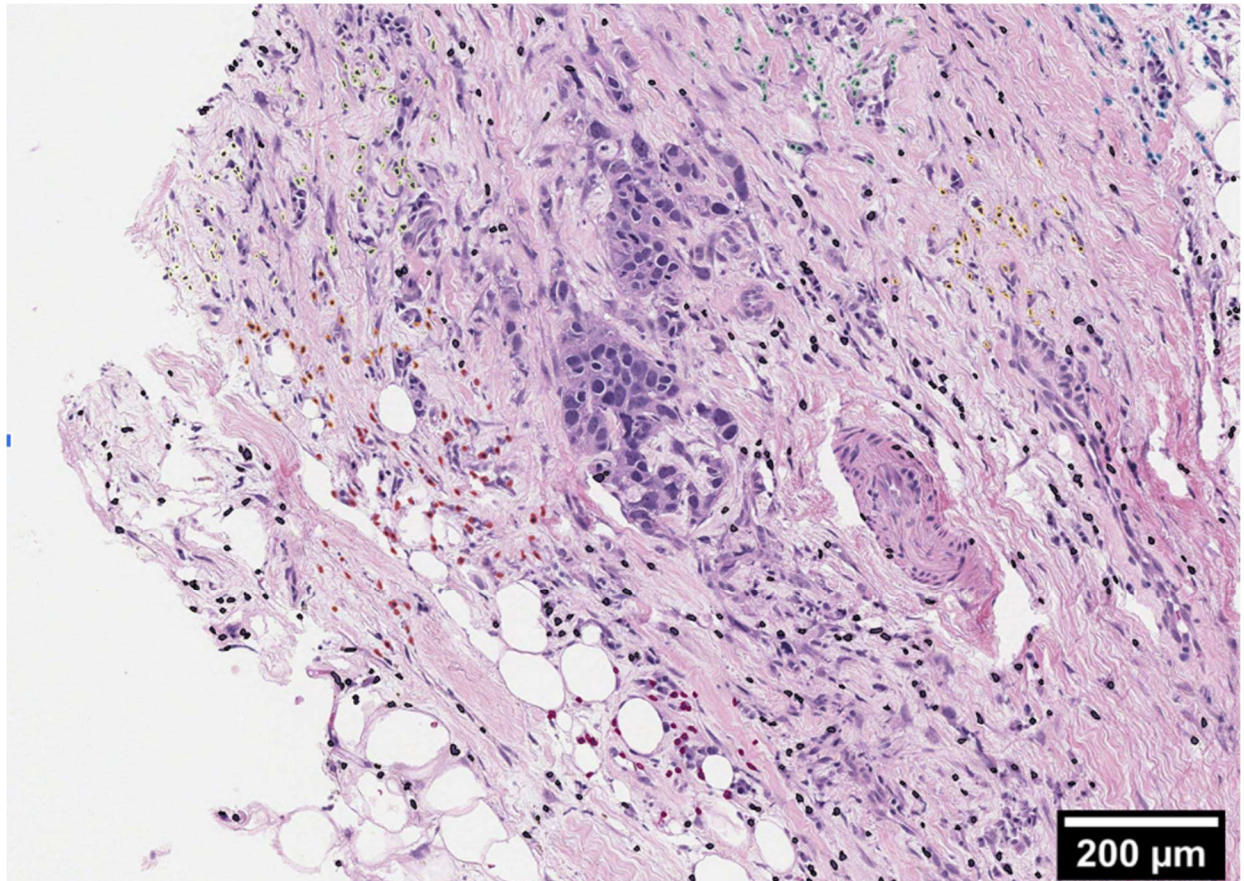


Figure 3.2: A patch overlaid with DBSCAN model fit on the filtered TIL cluster. 8 distinct clusters were recognized by the model indicating the potential for identification of TIL sub-types.

3. Scalability and Cloud Deployment: One of the key strengths of our pipeline is its focus on employing simple and efficient solutions for each step, enhancing its scalability. It is currently operated on an Nvidia GPU RTX 3060 in conjunction with a multi-core CPU. We are actively working towards deploying the pipeline on cloud infrastructure, which will enable seamless access and efficient processing of large-scale datasets from multiple institutions. Cloud deployment will facilitate broader adoption, collaboration, and streamlined integration into clinical workflows, accelerating the translation of automated TIL assessment into routine

practice, benefiting a wider range of patients through improved diagnostic and prognostic capabilities.

References

1. Saltz J, Gupta R, Hou L, et al. Spatial Organization and Molecular Correlation of Tumor-Infiltrating Lymphocytes Using Deep Learning on Pathology Images. *Cell Rep.* 2018;23(1):181-193.e7. doi: 10.1016/j.celrep.2018.03.086
2. Ribeiro JM, Mota JM, Sampaio C, Marques F, Gonçalves M, Amorim J. Triple-negative breast cancer: the current role of the tumor microenvironment. *Cancers (Basel).* 2022;14(5):1351.
3. Zagami, P., Carey, L.A. Triple negative breast cancer: Pitfalls and progress. *npj Breast Cancer* 8, 95 (2022). doi:10.1038/s41523-022-00468-0
4. Wu R, Oshi M, Asaoka M, et al. Intratumoral Tumor Infiltrating Lymphocytes (TILs) are Associated with Cell Proliferation and Better Survival But Not Always With Chemotherapy Response in Breast Cancer. *Ann Surg.* 2023;278(4):587-597. doi:10.1097/SLA.0000000000005954
5. Gonzalez H, Hagerling C, Werb Z. Roles of the immune system in cancer: from tumor initiation to metastatic progression. *Genes Dev.* 2018;32(19-20):1267-1284. doi:10.1101/gad.314617.118
6. Loi S, Drubay D, Adams S, et al. Tumor-Infiltrating Lymphocytes and Prognosis: A Pooled Individual Patient Analysis of Early-Stage Triple-Negative Breast Cancers. *J Clin Oncol.* 2019;37(7):559-569. doi:10.1200/JCO.18.01010
7. Ciarka A, Piątek M, Pęksa R, Kunc M, Senkus E. Tumor-Infiltrating Lymphocytes (TILs) in Breast Cancer: Prognostic and Predictive Significance across Molecular Subtypes. *Biomedicines.* 2024; 12(4):763. <https://doi.org/10.3390/biomedicines12040763>

8. Kazemi MH, Sadri M, Najafi A, et al. Tumor-infiltrating lymphocytes for treatment of solid tumors: It takes two to tango?. *Front Immunol.* 2022;13:1018962. Published 2022 Oct 28. doi:10.3389/fimmu.2022.1018962
9. Tine, Juul, Monberg., Troels, Holz, Borch., Inge, Marie, Svane., Marco, Donia. (2023). TIL Therapy: Facts and Hopes.. *Clinical Cancer Research*, doi: 10.1158/1078-0432.CCR-22-2428
10. Salgado R, Denkert C, Demaria S, et al. The evaluation of tumor-infiltrating lymphocytes (TILs) in breast cancer: recommendations by an International TILs Working Group 2014. *Ann Oncol.* 2015;26(2):259-271. doi:10.1093/annonc/mdu450
11. Hendry S, Salgado R, Gevaert T, et al. Assessing Tumor-infiltrating Lymphocytes in Solid Tumors: A Practical Review for Pathologists and Proposal for a Standardized Method From the International Immunooncology Biomarkers Working Group: Part 1: Assessing the Host Immune Response, TILs in Invasive Breast Carcinoma and Ductal Carcinoma In Situ, Metastatic Tumor Deposits and Areas for Further Research. *Adv Anat Pathol.* 2017;24(5):235-251. doi:10.1097/PAP.000000000000162
12. Klauschen F, Müller KR, Binder A, et al. Scoring of tumor-infiltrating lymphocytes: From visual estimation to machine learning. *Semin Cancer Biol.* 2018;52(Pt 2):151-157. doi:10.1016/j.semcancer.2018.07.001
13. Thaer Khoury, Xuan Peng, Li Yan, Dan Wang, Vidya Nagrale, Tumor-Infiltrating Lymphocytes in Breast Cancer: Evaluating Interobserver Variability, Heterogeneity, and Fidelity of Scoring Core Biopsies, *American Journal of Clinical Pathology*, Volume 150, Issue 5, November 2018, Pages 441–450, <https://doi.org/10.1093/ajcp/aqy069>

14. Thagaard J, Broeckx G, Page DB, et al. Pitfalls in machine learning-based assessment of tumor-infiltrating lymphocytes in breast cancer: A report of the International Immunology Biomarker Working Group on Breast Cancer. *J Pathol.* 2023;260(4):498-513. doi:10.1002/path.6155.
15. Bai Y, Cole K, Martinez-Morilla S, et al. An Open-Source, Automated Tumor-Infiltrating Lymphocyte Algorithm for Prognosis in Triple-Negative Breast Cancer. *Clin Cancer Res.* 2021;27(20):5557-5565. doi:10.1158/1078-0432.CCR-21-0325.
16. Zixiao Lu et al., Deep-Learning–Based Characterization of Tumor-Infiltrating Lymphocytes in Breast Cancers From Histopathology Images and Multiomics Data. *JCO Clin Cancer Inform* 4, 480-490(2020). DOI:10.1200/CCI.19.00126
17. Choi, S., Cho, S.I., Jung, W. et al. Deep learning model improves tumor-infiltrating lymphocyte evaluation and therapeutic response prediction in breast cancer. *npj Breast Cancer* 9, 71 (2023). <https://doi.org/10.1038/s41523-023-00577-4>
18. Lim SM, Park HL, Hwang S, et al. Artificial intelligence-powered spatial analysis of tumor-infiltrating lymphocytes in colon cancer. *NPJ Precis Oncol.* 2023;7(1):11. doi:10.1038/s41698-023-00470-0
19. Mohammad, Yosofvand., Sonia, Y., Khan., Rabin, Dhakal., Ali, Nejat., Naima, Moustaid-Moussa., Rakhshanda, Layeequr, Rahman., Hanna, Moussa. (2023). Automated Detection and Scoring of Tumor-Infiltrating Lymphocytes in Breast Cancer Histopathology Slides. *Cancers*, doi: 10.3390/cancers15143635
20. Mohammed, Hassouna., Mohammad, T., Al-Antary., Mohammed, Ali, Saleh., Nedaa, Baker, Al, Barghuthi. (2023). Applications of Deep Learning in Medical Imaging: A Brief Review. doi: 10.1109/ASET56582.2023.10180645

21. Yoichi, Hayashi. (2019). Black Box Nature of Deep Learning for Digital Pathology: Beyond Quantitative to Qualitative Algorithmic Performances. doi: 10.1007/978-3-030-50402-1_6
22. Corredor G, Wang X, Zhou Y, et al. Spatial Architecture and Arrangement of Tumor-Infiltrating Lymphocytes for Predicting Likelihood of Recurrence in Early-Stage Non-Small Cell Lung Cancer. Clin Cancer Res. 2019;25(5):1526-1534. doi:10.1158/1078-0432.CCR-18-2013
23. Yuan Y. 2015 Modelling the spatial heterogeneity and molecular correlates of lymphocytic infiltration in triple-negative breast cancer. J. R. Soc. Interface 12: 20141153. <http://dx.doi.org/10.1098/rsif.2014.1153>
24. Jain AK. Data clustering: 50 years beyond K-means. Pattern Recognition Letters. 2010;31(8):651-666. doi:10.1016/j.patrec.2009.09.011.
25. Krizhevsky A, Sutskever I, Hinton GE. ImageNet classification with deep convolutional neural networks. Commun ACM. 2017;60(6):84-90. doi:10.1145/3065386.
26. Ravikanth M, Soujanya P, Manjunath K, Saraswathi TR, Ramachandran CR. Heterogeneity of fibroblasts. J Oral Maxillofac Pathol. 2011;15(2):247-250. doi:10.4103/0973-029X.84516